Stony Brook University

The official electronic file of this thesis or dissertation is maintained by the University Libraries on behalf of The Graduate School at Stony Brook University.

Exploring RNA Binding Pattern of Rim4 in Meiosis

A Thesis Presented

by

Che Xiao

to

The Graduate School

in Partial Fulfillment of the

Requirements

for the Degree of

Master of Arts

in

Biological Sciences

Stony Brook University

August 2014

Stony Brook University

The Graduate School

Che Xiao

We, the thesis committee for the above candidate for the
Master of Arts degree, hereby recommend
acceptance of this thesis.

Bruce Futcher – Thesis Advisor
Professor, Department of Molecular Genetics and Microbiology

Aaron Neiman – Second Reader
Professor, Department of Biochemistry and Cell Biology

This thesis is accepted by the Graduate School

Charles Taber
Dean of the Graduate School

Abstract of the Thesis

Exploring RNA Binding Pattern of Rim4 in Meiosis

by

Che Xiao

Master of Arts

in

Biological Sciences

Stony Brook University

2014

In *Saccharomyces cerevisiae*, translation is regulated in meiosis [1]. Rim4 is an RNA binding protein with two RNA recognition motifs (RRMs). Previous studies [2] have shown that point mutations in either RRM knock out the translational repression of *CLB3, SPO20, GIP1* and *SPS1* in meiosis I, suggesting that the translational control of these genes may be due to Rim4. We wished to see the full range of RNAs bound by Rim4. We applied RIP-chip (RNA Immunoprecipitation/microarray) and CLIP-seq (*in vivo* Crosslinking and Immunoprecipitation/sequencing) to identify the RNAs co-immunoprecipitated with Rim4 in a synchronized meiosis I culture. The translationally-repressed genes co-clustering with *CLB3*, and translationally-repressed genes co-clustering with *AMA1* in ribosome footprint data [1] were enriched in Rim4 immunoprecipitates compared to the negative controls. Therefore, these two groups of translationally repressed genes seem to be the targets of Rim4. Some other genes without translational repression in meiosis I were also enriched in Rim4 immunoprecipitates.

Table of Contents

List of Figures

List of Tables

List of Abbreviations

m6A, N^6- methyladenosine

RRM, RNA recognition motif

TAP, Tandem affinity purification

IP, immunoprecipitation

RIP-chip, RNA Immunoprecipitation/microarray

CLIP-seq, *in vivo* Crosslinking and Immunoprecipitation/sequencing

qPCR, quantitative Polymerase Chain Reaction

Acknowledgement

Chapter 1

Introduction

1.1 Overview of yeast meiosis

Meiosis is a specialized pathway where a diploid cell undergoes DNA replication once and nuclear division twice to finally generate four haploid gametes. Budding yeast *Saccharomyces cerevisiae* is a good model to study meiosis. As one of the simplest eukaryotic organisms, *cerevisiae* can execute either mitosis or meiosis, depending on environment. In rich media, cells replicate themselves through mitosis. Upon deprivation of nitrogen and fermentable carbon source, diploid cells will go through meiosis and form spores.

The meiotic process is delicately regulated to ensure all the events happen in the right order. Yeast meiotic regulation at the transcriptional level has been studied for the last decade [3–6]. There are several major transcriptional waves in meiosis (Figure 1). Based on the transcription timing, genes expressed in meiosis are roughly grouped into four categories: early, middle, mid-late and late genes. Early genes are mostly involved in meiotic prophase, facilitating homologous chromosome pairing and recombination. Ime1 is the master regulator of early genes. Ime1 and other early genes turn on the expression of Ndt80, which activates the expression of middle genes. Middle genes are mainly responsible for meiotic division and spore formation. The expression of mid-late and late genes is turned on later in sequential order. Mid-late genes are involved in spore wall formation, while the late genes are responsible for spore maturation [3].

Meiosis is also regulated at the post-transcriptional level. In meiosis, this regulation might be even more prevalent than the transcriptional regulation. In principle, after being transcribed, RNA could be modified and regulated in various ways. RNA stability, RNA localization, translation and splicing are the commonly regulated aspects. Several post-transcriptionally regulated cases have been reported in yeast meiosis. First, many genes, including *CLB3, SPO20,* etc, have been found to exhibit delayed translation in middle meiosis [1,2]. Second, RNA N^6- methyladenosine (m6A) modification is only present in meiotic transcripts, but not in vegetative transcripts [7–10], suggesting an important role of m6A in meiosis. Mammalian m6A has been found to affect RNA stability and localization [11,12]. Yeast m6A modification may also function in similar ways.

Post-transcriptional regulation is usually achieved with the help of RNA binding proteins. Therefore, investigating meiotic RNA binding proteins will be a good starting point to understand post-transcriptional regulation in meiosis.

1.2 Overview of Rim4

Rim4 is a meiosis specific protein with two RNA recognition motifs (RRMs) (Figure 2). Therefore, it might be able to bind RNA. Cells lacking Rim4 have complete defect in sporulation, but no obvious growth defect in YPD, YPA or synthetic media [13].

Rim4 is an important player in early meiosis. Rim4 expression is induced in early meiosis, and dependent on Ime1. Homozygous *rim4* null mutation leads to a reduction in the level of *IME2* transcript [14]. The *rim4Δ* homozygous mutant is defective in premeiotic DNA synthesis.

A *rim4Δ sic1 Δ* double mutant can undergo DNA synthesis, but fails to complete normal sporulation [13], suggesting that Rim4 might be also involved in middle or late meiosis.

Recently, Rim4 was found to mediate translational regulation in middle meiosis [2]. At the onset of meiosis I, a group of genes, including *CLB3, GIP1*, etc., is transcribed with the activation of Ndt80. However, these transcripts will not be translated until meiosis II. Berchowitz *et al* demonstrated that this translational repression is mediated directly or indirectly by Rim4. When the conserved phenylalanine in each of the two RRMs of Rim4 is replaced by leucine (F349L/F139L), the translational repression of *CLB3* no longer exists. Clb3 protein expression then mirrors its RNA expression pattern (Figure 3). In addition, Rim4 protein has been pulled down by *in vitro* transcribed *CLB3* RNA, supporting the idea that Rim4 directly binds *CLB3* to regulate its translation.

1.3 Goal of this work

Based on the work done by Berchowitz *et al*, we hypothesized that the translational control of *CLB3* and many other genes were mediated by Rim4 through direct binding in meiosis I. As a very abundant protein in meiosis, Rim4 might bind many transcripts. However, the only well-established target of Rim4 was *CLB3*, and this could not explain the phenotypes of *rim4* mutants in early meiosis. So we were very curious to know other binding targets of Rim4 and to find a full target list for Rim4. Therefore, we wanted to immunoprecipitate Rim4 from meiosis I cells and identify its transcriptome-wide targets by high-throughput methods. This work might help to deepen our understanding of post-transcriptional regulation in yeast meiosis.

Chapter 2

Materials and Methods

2.1 Strains

The yeast strains used in this study are listed in Table 1. All the strains were in the SK1 background, which had high sporulation efficiency. In order to increase culture synchrony, a *GAL-NDT80* inducible cassette [15] was included in all the strains. In this *GAL4.ER pGAL-NDT80* construction, *NDT80* was placed under the promoter of *GAL1-10*, while a fusion Gal4.ER protein was expressed. Without β-estradiol, Ndt80 protein was not expressed. As a result, cells entering meiosis would be arrested at pachytene stage. Upon addition of β-estradiol, Gal4.ER fusion protein would enter the nucleus and activate the expression of Ndt80 from *Gal1-10* promoter. Arrested cells then continued to do meiosis in good synchrony.

Homozygous wild-type untagged Rim4 diploid strains (A14201, A15055), homozygous wild-type 3×V5 tagged Rim4 diploid strain (A30868), and homozygous 1st RRM domain mutated (*F139L*) 3×V5 tagged diploid *rim4* strain (A31420) were generous gifts from Dr. Amon's lab. CX6 was a homozygous wild-type TAP tagged Rim4 diploid strain. TAP-kanMX6 cassette was PCR-amplified from the plasmid pFA6a-CBP 2×protein A (TEV)-kanMX6, and integrated at the C-terminus of Rim4 right before the stop codon by homologous recombination. Haploid wild-type TAP tagged Rim4 strains of opposite mating types were crossed to produce diploid strain CX6.

2.2 Synchronized sporulation condition

Yeast strains with *GAL4.ER pGAL-NDT80* cassette were induced to undergo synchronized sporulation as in the protocol described previously [15] with minor modifications. Cells were first cultured on YPD (1% yeast extract, 2% peptone and 2% glucose) plates at 30°C overnight. Cells were then transferred to YPD liquid medium and grown to saturation. After that, cells were washed with H_2O, inoculated 1:100 in BYTA medium (1% yeast extract, 2% tryptone, 1% potassium acetate, 50 mM potassium pthalate) to $OD_{600} \approx 0.18$ and grown at 30°C for another 14h until $OD_{600} \approx 1.2$. Cells were then washed with SPO medium (1% potassium acetate) twice, and resuspended in SPO with final $OD_{600} \approx 1.9$. Cells were further incubated in SPO at 30°C for 6h, and became arrested at the Ndt80 block. When β-estradiol was added to a final concentration of 1 μM at 6h, the Ndt80 block was released and cells continued meiotic progression synchronously.

2.3 DAPI staining

1 mL cell culture was immediately fixed in 100 μL 37% formaldehyde. Cells were washed and strained with 1 μg/mL DAPI. Meiotic stage of harvested cells was assayed by fluorescence microscopy.

2.4 Western blotting

Proteins were first separated by 10% SDS-PAGE electrophoresis, and transferred to PVDF membrane in wet condition with constant current of 400 mA at 4°C for 1.5h. Ponceau

S staining was performed to reversibly detect proteins on the membrane. Membrane was then blocked with 5% non-fat milk for 1h at room temperature.

Different antibodies were chosen to bind proteins with different tags. (1) To detect TAP tagged protein, membrane was incubated with 1:5,000 diluted Peroxidase Anti-Peroxidase (PAP) soluble complex (Sigma cat# P1291) in 5% non-fat milk. (2) In order to detect 3×V5 tagged protein, membrane was first incubated with 0.5 μg/mL anti-V5 antibody (GenScript, cat# A01724-100) in TBST (20 mM Tris [pH 7.5], 500 mM NaCl, 0.1% Tween 20) at 4°C overnight, washed, and then incubated with 1:20k HRP-conjugated goat-anti-mouse secondary antibody in 1% non-fat milk for 1h at room temperature.

Enhanced chemiluminescence (ECL) substrate (Bio-Rad, cat# 170-5060) was applied to detect desired proteins.

2.5 RNA Immunoprecipitation/microarray (RIP-chip) experiments

RIP-chip experiments were performed as described previously (Hogan et al. 2008; Cai and Futcher 2013) with modifications.

2.5.1   Cell harvesting

A15055 (wild-type untagged Rim4, *RIM4*), A30868 (wild-type 3×V5 tagged Rim4, *RIM4-3V5*) and A31420 (1st RRM mutated 3×V5 tagged *rim4*, *rim4-F139L-3V5*) were used in RIP-chip experiments. For each strain, 800mL cells (OD_{600} =1.9) were harvested at 7.5h,

when meiosis I cell percentage peaked [2]. Cells were snap-frozen in liquid nitrogen, and stored at -80°C.

2.5.2 RIP-chip

Cells were thawed on ice, and resuspended in lysis buffer (10 mM HEPES-Na [pH 7.5], 50 mM KCl, 1.5 mM MgCl$_2$, 0.5 mM DTT, 100 U/mL Ribolock RNase inhibitor (Fisher Scientific, cat# FEREO0382), 0.2 mg/mL heparin, 20 U/mL DNase I, 5 µg/mL pepstatin A, 2×Roche complete EDTA-free protease inhibitor cocktail (Roche, cat# 11873580001), 50 nM staurosporine). Cells were lysed by zirconium bead beating in a FastPrep, with lysis efficiency >90%. 1% Triton X-100 was added to each tube and mixed. Cell lysate was transferred to a new tube, and centrifuged at 14,000 rpm for 10 min. The supernatant was collected, and incubated with IgG-Sepharose beads (GE Healthcare, cat# 17-0969-01) for 15 min to pre-clear the extract. After centrifuging at 1,000 rpm for 1 min, supernatant was collected again, and incubated with anti-V5 agarose beads (Sigma, cat# A7345) for 1h. Beads then underwent three washes with high salt wash buffer (10 mM Hepes-Na [pH 7.5], 75 mM KCl, 1.5 mM MgCl$_2$, 0.5 mM DTT, 100 U/mL Ribolock RNase inhibitor, 0.2 mg/mL heparin, 5 µg/mL pepstatin A, 2×Roche complete EDTA-free protease inhibitor cocktail), and then three washes with low salt wash buffer (10 mM Hepes-Na [pH 7.5], 10 mM KCl, 1.5 mM MgCl$_2$, 0.5 mM DTT, 100 U/mL Ribolock RNase inhibitor, 5 µg/mL pepstatin A, 2×Roche complete EDTA-free protease inhibitor cocktail). 3×V5 tagged proteins were eluted from the beads with 2.5 mg/ml V5 peptide (Sigma, V7754) in 30 µL elution buffer (10mM HEPES-Na [pH 7.5], 1.5mM MgCl$_2$, 0.25mM EDTA, 20% glycerol, 30mM KCl, 0.3% NP-40, 5 µg/mL pepstatin A, 2×Roche complete EDTA-free protease inhibitor cocktail, 100 U/mL Ribolock

7

RNase inhibitor) at 4°C for 10 min and at room temperature for another 10 min. The elution

step was repeated once. Both eluates were pooled, and SDS was added to a final

concentration of 0.5%. RNA in this solution was purified with phenol/chloroform/isoamyl

alcohol (25:24:1) extraction twice, followed by chloroform extraction once and ethanol

precipitation. The RNA pellet was resuspended in RNase-free water, and served as

experimental RNA for microarray preparation. Total RNA from A30868 (wild-type 3×V5

tagged Rim4, *RIM4-3V5*) was extracted by RiboPure™-Yeast Kit (LifeTechnologies, cat#

AM1926), and served as reference RNA in the next step.

Experimental and reference RNAs were reverse transcribed to cDNA by random

hexamers with SuperScript III (LifeTechnologies, cat# 18080044), and converted to cRNA

labelling with Cy3 or Cy5, respectively. Both Cy3 and Cy5 cRNAs were hybridized to

Agilent 8x15K expression arrays. Cy3 (green) and Cy5 (red) intensities for each microarray

spot were obtained from scanning results.

For a particular gene, RNA enrichment was calculated as the ratio of Cy3 intensity over

Cy5 intensity, which revealed the ratio of immunoprecipitated RNA over total RNA. RNA

enrichment was then normalized by *GAL* genes. The median enrichment of five highly

expressed *GAL* genes (*GAL1*, *GAL2*, *GAL4*, *GAL7*, and *GAL10*) was used as the

normalization factor. Therefore, the formula for calculating the normalized RNA enrichment

was:

$$enrichment_{(Gene\ X, normalized)} = \frac{Cy3}{Cy5}\ ratio_{(Gene\ X)} / \frac{Cy3}{Cy5} ratio_{(median\ of\ 5\ Gal\ genes)}$$

There were two ways to determine RNA specific enrichment of a particular gene, since two negative control strains were used in the parallel experiments. Normalized RNA enrichment from the wild-type tagged Rim4 strain could be (1) compared with that of wild-type untagged Rim4strain, as shown in the formula:

$$specific\ enrichment_{(Gene\ X)} = \frac{enrichment_{(WT\ tag,\ normalized,\ Gene\ X)}}{enrichment_{(WT\ untag,\ normalized,\ Gene\ X)}}$$

(2) Or, compared to 1st RRM mutated tagged *rim4* strain, as shown in the formula:

$$specific\ enrichment_{(Gene\ X)} = \frac{enrichment_{(WT\ tag,\ normalized,\ Gene\ X)}}{enrichment_{(Mutant\ tag,\ normalized,\ Gene\ X)}}$$

We were particularly interested in the specific enrichment of the following groups of genes:

(1) Genes co-clustering with *CLB3* in the Brar footprint data [1]:

CLB3, GIP1, SPS1, YSP2, YFL012W, and *SPO20*

(2) Genes co-clustering with *AMA1* in the Brar footprint data [1]:

AMA1, HXT10, SPR6, YGL230C, YLR049C, SGA1, ECM8, ECM23, PIG2, FRA1, CDC27, CTS2, SSP2, YDR042C, YOR214C, UBC11, YPR077C, YPR078C

(3) (Negative control) Genes strongly expressed and translated after *NDT80* expression; co-cluster with *CDC5* in the Brar footprint data [1]:

YDL186W, CLB4, YJL043W, YML199W, YBR250W, YEH1, YJR107W, SPO12,

TEP1, SPO75, HST3, TIM18, YGL138C, SGO1, YOL047C, MUM3, YKR005C,

YAL018C, PES4, HST1, SPO21, YOR024W, TID3, CDC5, STO1, CBC2

A two-tailed t-test was performed to examine the difference between translationally repressed genes (Group (1) and Group (2)) and negative control pool (Group (3)).

2.6 *in vivo* Crosslinking and Immunoprecipitation/sequencing (CLIP-seq) experiments

CLIP-seq experiments were performed as described previously [18,19] with modifications.

2.6.1 Cell harvesting

A14201 (wild-type untagged Rim4, *RIM4*), CX6 (wild-type TAP tagged Rim4, *RIM4-TAP*) were used in CLIP-seq experiments.

For each strain, 50 mL meiosis I (7.5 h) cells were cross-linked before harvesting. Two types of cross-linking methods were performed. (1) Formaldehyde cross-linking. Formaldehyde was added to the cell culture (final concentration 1%), mixed, and incubated on ice for 15 min. Glycine was then added to a final concentration of 1 M and incubated for additional 5 min, in order to stop the cross-linking reaction. (2) UV cross-linking. Cells were washed with H_2O and resuspended in 50 mL H_2O. Cell suspension was then transferred to three 100×15mm petri dishes, with ~17 mL suspension each. Each petri dish was irradiated with 254 nm UV from the distance of 15 cm in UV Stratalinker 1800. At the "Energy" mode

of the cross-linker, three different UV dosages were set to apply to cell suspension respectively: 2,000 mJ/cm^2 (low), 10,000 mJ/cm^2 (mid), or 50,000 mJ/cm^2 (high). It was noteworthy that the UV dosage setting might not reflect the actual UV exposure to each cell suspension, since we did not find a UV calibrator to correct machine error. Alternatively, we performed a cell viability assay to estimate the power of our UV cross-linker. ~80% of cells were killed at the dosage setting of 10,000 mJ/cm^2 (mid).

Cross-linked cells were collected in a centrifuge tube and spun down. After DEPC-treated H$_2$O wash twice, cell pellets were snap-frozen in liquid nitrogen, and stored at -80°C.

2.6.2 CLIP- Seq

Cells were thawed on ice, and resuspended in 500 μL lysis buffer (50 mM HEPES-Na [pH 7.5], 140 mM NaCl, 0.5 mM DTT, 100 U/mL Ribolock RNase inhibitor (Fisher Scientific, cat# FEREO0382), 0.2 mg/mL heparin, 5 μg/mL pepstatin A, 2 μg/mL leupeptin, 2 μg/mL aprotinin, 1 mM PMSF, 2×Roche complete protease inhibitor cocktail (Roche, cat# 11697498001)). Cells were lysed by zirconium bead beating in a FastPrep, with lysis efficiency >90%. 0.1% sodium deoxycholate and 1% Triton X-100 were added to each tube and mixed. Cell lysate was transferred to a new tube, sonicated briefly (two 15s pulse of 50% amplitude, with 1 min cooling down on ice in between), and centrifuged at 14,000 rpm for 10 min. Supernatant was collected, of which 50 μL was saved as "input" sample, and the rest "IP" sample was incubated with pre-washed IgG Sepharose beads (GE Healthcare, cat# 17-0969-01) for 1h. Beads then underwent three washes with FA500 buffer (50 mM HEPES-Na [pH 7.5], 500 mM NaCl, 0.1% sodium deoxycholate, 1% Triton X-100, 0.1% SDS, 100

U/mL Ribolock RNase inhibitor (Fisher Scientific, cat# FEREO0382), 0.2 mg/mL heparin, 5

µg/mL pepstatin A, 2 µg/mL leupeptin, 2 µg/mL aprotinin, 1 mM PMSF, 2×Roche complete

protease inhibitor cocktail (Roche, cat# 11697498001)), and then two washes with LiCl

buffer (10 mM Tris-Cl [pH 8.0], 250 mM LiCl, 0.1% sodium deoxycholate, 0.5% NP-40,

100 U/mL Ribolock RNase inhibitor (Fisher Scientific, cat# FEREO0382), 5 µg/mL

pepstatin A, 2 µg/mL leupeptin, 2 µg/mL aprotinin, 1 mM PMSF, 2×Roche complete

protease inhibitor cocktail (Roche, cat# 11697498001)). Tagged proteins were eluted from

beads by incubating in 50 µL RIP buffer (1 mM EDTA, 1% SDS, 40 mM Tris-Cl [pH 8.0],

100 U/mL Ribolock RNase inhibitor (Fisher Scientific, cat# FEREO0382)) at 65°C for 5 min,

and the elution was repeated once. Both eluates were pooled, treated with 0.2 µg/µL

proteinase K at 42°C for 1h. "Input" samples underwent proteinase K treatment in parallel.

For formaldehyde cross-linked samples, additional reverse cross-linking incubation at 70°C

for 30 min was performed. RNA from both "IP" and "input" samples were purified with

phenol/chloroform/isoamyl alcohol (25:24:1) extraction twice, followed by chloroform

extraction once and ethanol precipitation. After DNase (Ambion, cat# AM2238) treatment,

RNA samples were stored at -80°C for the next step.

To examine RNA enrichment by quantitative PCR (qPCR), RNA was reverse transcribed

to cDNA by random hexamers with SuperScript III (LifeTechnology, cat# 18080044). Six

genes were examined. *SPO20, CLB3, YFL012W* were the genes with delayed translation and

potential targets of Rim4. *CDC5, PES4, GAL7* were the genes without obvious delayed

translation and served as negative controls. qPCR primers for each gene are listed in Table 2.

For each gene, RNA enrichment was calculated as the ratio of its cDNA amount of "IP"

sample in wild-type tagged Rim4 strain divided by that of wild-type untagged strain, as shown in the formula below:

$$enrichment_{(Gene\ X)} = \frac{cDNA\ amount_{(WT\ tag,\ IP,Gene\ X)}}{cDNA\ amount_{(WT\ untag,IP,\ Gene\ X)}}$$

To examine global RNA enrichment by sequencing, RNA was converted to a sequencing library using Ovation Universal RNA-Seq kit (NuGEN, cat# 0343-32). In particular, RNA was reverse transcribed to 1st strand cDNA by random hexamers. Libraries were loaded on flow cell, and run on a MiSeq with MiSeq v3 reagent-150 cycle (Illumina, cat# MS-102-3001). Reads were mapped to *Saccharomyces cerevisiae* genome by Bowtie 2. Reads per gene were counted. To avoid 0 in the denominator in the future analysis, 1 was added to each read count. Corrected read count was normalized in per million reads. RNA enrichment can be calculated in two ways.

(1) RNA enrichment of a particular gene was calculated as the ratio of its reads in "IP" sample divided by reads in "input" sample. Both samples are from wild-type tagged Rim4 strain, as shown in the formula below:

$$enrichment_{(Gene\ X)} = \frac{Reads_{(WT\ tag,\ IP,Gene\ X)}}{Reads_{(WT\ tag,input,\ Gene\ X)}}$$

(2) RNA enrichment of a particular gene was calculated as the ratio of its reads in "IP" sample from wild-type tagged Rim4 strain divided by reads in "IP" sample from wild-type untagged strain, as shown in the formula below:

$$enrichment_{(Gene\ X)} = \frac{Reads_{(WT\ tag,\ IP,Gene\ X)}}{Reads_{(WT\ untag,IP,\ Gene\ X)}}$$

The same set of pre-selected genes was used as in RIP-chip experiment analysis. A two-tailed t-test was performed to examine the differences between translationally repressed genes and the negative control pool.

Chapter 3

Results

3.1 RNA Immunoprecipitation/microarray (RIP-chip) experiments

To identify RNAs co-immunoprecipitated with Rim4, RIP experiments were performed

on meiosis I cells from a wild-type 3×V5 tagged Rim4 strain. The same procedure was done

in parallel on meiosis I cells from wild-type untagged Rim4 strain and 1st RRM mutated

(F139L) 3×V5 tagged *rim4* strain, as negative controls. For experimental details, please refer

to the Materials and Methods section.

Western blotting results (Figure 5A) showed that 3×V5 tagged Rim4 was successfully

pulled down in wild-type 3×V5 tagged Rim4 strain and 1st RRM mutated tagged *rim4* strain,

while no protein band of the expected size was present in the untagged control strain.

Proteins of smaller sizes were also present in both tagged strains. These might be Rim4

protein degradation products, although protease inhibitors, including pepstatin A and Roche

complete protease inhibitor cocktail, had been applied throughout the RIP procedure.

Microarrays were used to examine all the RNAs in Rim4 immunoprecipitates. We were

particularly interested in three groups of genes. Their RNA expression patterns (Xu and

Futcher, unpublished data) and ribosome footprint pattern [1] during meiotic progression are

illustrated in Figure 4. The three pre-selected groups of genes were: (1) translationally

repressed genes co-clustering with *CLB3* in the Brar footprint data; (2) translationally

repressed genes co-clustering with *AMA1* in the footprint data; (3) (negative control) genes

15

strongly expressed and translated after *NDT80* expression, and co-clustering with *CDC5* in the footprint data.

There were two ways to determine RNA specific enrichment of a particular gene, since two negative control strains were used in the parallel experiments. We first investigated the specific enrichment by comparing RNA immunoprecipitated from the wild-type tagged Rim4 strain, with RNA from wild-type untagged Rim4 strain (Figure 5B, Table 3). The enrichment scores of translationally repressed gene group (genes co-clustering with *CLB3* and genes co-clustering with *AMA1* together as a pool, i.e., Group (1) plus Group (2)) were significantly higher than the group of negative control genes (p= 0.02). In particular, *SPO20* ranked 3rd on the top enriched RNA list. These results suggested that translationally repressed genes are the binding targets of Rim4. This is consistent with *in vitro* RNA pull down experiments [2], and supported the hypothesis that Rim4 directly binds these genes to regulate their translation.

We then investigated the specific enrichment by comparing RNA immunoprecipitated from the wild-type tagged Rim4 strain, with RNA from RRM mutated tagged *rim4* strain (Figure 5C). We observed significant higher enrichment of translationally repressed gene group, than that of the negative control gene group (p = 1.57E-07). These results also supported the idea that those translationally repressed genes are the binding targets of Rim4.

We also noticed that the latter comparison with RRM mutant tagged strain had a much smaller p-value (p = 1.57E-07) than the former comparison with wild-type untagged strain (p = 0.02). Figure 5C also exhibited a much more separated enrichment pattern between translationally repressed genes and negative controls, than Figure 5B. It suggested that the

comparison with RRM mutant tagged strain had better specificity. However, there was a concern whether it was appropriate to compare the wild-type strain and mutant strain harvested at the same time point. A *rim4* RRM mutant strain entered meiosis I with a delay and decreased percentage of cells in meiosis I[2]. In other words, the majority of mutant strain cells harvested at 7.5h, when meiosis I cell percentage peaked in wild-type strain, were actually in an earlier meiotic stage before meiosis I. Then, it would be incorrect to directly compare Rim4 wild-type strain and mutant strain harvested at the same time.

Given the concern mentioned above, the specific enrichment by comparing RNA immunoprecipitated from the wild-type tagged Rim4 strain with RNA from wild-type untagged Rim4 strain was a more reasonable evaluation. But in this comparison, the p-value for the difference was only 0.02. While this is statistically significant, it is still not as small a p-value as one might hope. A single gene from the "enriched" genes did not always show a higher enrichment score than a single gene from the "control" genes. In other words, given a particular random gene, we could not confidently determine whether or not the gene was the target of Rim4 solely based on the RIP-chip data. In order to increase the specificity of RIP experiments, we tried to optimize various factors, including salt and detergent concentration, in the RIP procedure. But as the bead washing steps became more stringent, almost all the RNAs were washed away, and signal in the microarrays was lost. Therefore, we decided to switch to CLIP (*in vivo* Crosslinking and Immunoprecipitation) to allow more stringent washes, and perhaps increase the specificity.

3.2 *in vivo* Crosslinking and Immunoprecipitation/sequencing (CLIP-seq) experiments

CLIP procedure has several advantages over RIP. In CLIP, RNA is covalently linked

with its binding protein. The covalent bond stabilizes transient or weak interactions between

RNA and protein, enabling very stringent washes after immunoprecipitation [20]. In this way,

experiment specificity could be increased.

We performed CLIP experiments on meiosis I cells from a wild-type TAP tagged Rim4

strain, to identify RNAs co-immunoprecipitated with Rim4. The same procedure was done

on meiosis I cells from a wild-type untagged Rim4 strain in parallel as a negative control. For

experimental details, please refer to the Materials and Methods section.

Western blotting results (Figure 6A) showed that TAP tagged Rim4 was successfully

pulled down from the TAP tagged Rim4 strain, while no protein band of the expected size

was present in the untagged control strain. Proteins of smaller sizes were also present in the

tagged strain. It might be Rim4 protein degradation products, although various protease

inhibitors, including PMSF, pepstatin A, leupeptin, aprotinin and Roche complete protease

inhibitor cocktail, had been applied throughout the CLIP procedure.

We first did quantitative PCR (qPCR) to look at the RNA enrichment of several genes.

SPO20, CLB3, YFL012W were the genes with delayed translation and potential targets of

Rim4. *CDC5, PES4, GAL7* were the genes without obvious delayed translation and served as

negative controls. Translationally repressed genes were expected to have higher RNA

enrichment than the negative controls. As shown in Figure 6B, in most cases, we did observe

higher enrichment of translationally repressed genes *SPO20, CLB3, YFL012W* (left three bars

in each group), than the negative controls *CDC5, PES4, GAL7* (right three bars in each

group). In the formaldehyde cross-linking group, compared to untagged strain, *SPO20, CLB3,*

18

YFL012W were 31, 29 and 45 times enriched in tagged strain, while *CDC5, PES4, GAL7* were 22, 5 and 53 times enriched. *CDC5* and *GAL7* had near or even higher enrichment than potential target genes. In all the three UV treated groups, no matter what UV dosage was applied, the enrichment scores of translationally repressed genes were always higher than negative control genes.

Next, we wanted to further investigate the global RNA enrichment pattern of Rim4. We performed sequencing on the same materials from UV-mid group shown in Figure 6B. We sequenced both input and IP samples in both tagged and untagged strains. To be specific, input sample was the total RNA extracted from cell lysate prior to immunoprecipitation, while IP (immunoprecipitated) sample was the RNA co-immunoprecipitated with tagged protein.

The sequencing quality of the four samples was good. Input samples from both tagged and untagged strains had good alignment rate to *Saccharomyces cerevisiae* genome (98.12% and 97.99%, respectively). However, in the IP samples, only 51.51% of the reads from tagged strain were aligned to yeast genome, and 2.12% of the reads from the untagged strain were aligned. We were curious as to the reason for such poor alignment. Since the poorly-aligned IP samples were loaded on the same flow cell with the well-aligned input samples, the poor alignment was unlikely to come from technical problems of running the sequencer. We then randomly surveyed 20 unmapped reads from the two IP samples. Some (~30%) of the unmapped reads were matched to other species in the database (*Homo sapiens, Propionibacterium acnes*, pig, etc). These might be contamination in the experiments; it is strange that they should outnumber the yeast reads. Even stranger, most of unmapped reads could not be matched to any species in the PubMed database. Indeed, it could be a good sign

that CLIP worked really well. If the majority of nonspecific binding RNA was washed away from beads in CLIP, we would not extract much RNA in the end. Particularly for the untagged strain, in the perfect scenario, all the non-specific RNA was washed away and no RNA could be finally extracted. In this case, random environmental contaminants might dominate the PCR step in library preparation. Then only a small proportion of library truly came from Rim4 CLIP experiments, while the majority was random contamination. However, we could not exclude other unknown possibilities that might actually lead to the poor alignment of IP samples.

We then decided to analyze MiSeq data based on the mapped reads. Reads per gene were counted and normalized in per million reads. There were at least two ways to calculate the RNA enrichment of a specific gene. (1) RNA enrichment could be calculated as the ratio of the reads in IP sample over the reads in input sample. Both samples are from wild-type tagged Rim4 strain. (2) RNA enrichment could also be calculated as the ratio of the reads in IP sample from wild-type tagged Rim4 strain over that of wild-type untagged strain. Theoretically, method (2) would reveal a more specific RNA binding pattern of Rim4, because method (1) could not remove the background noise which came from the nonspecific RNA binding to the beads and protein complexes. But in our case, the reliability of method (2) might be a concern, because the two datasets used were the IP samples from the tagged and untagged strains, both of which were poorly aligned (51.51% and 2.12%, respectively). In method (1), the two datasets used were the better aligned (51.51%) tagged IP sample and the well-aligned (98.12%) tagged input sample. Therefore, the result from method (1) was more reliable, but perhaps less specific.

Figure 6C and 6D illustrated the global RNA enrichment in Rim4 CLIP experiments, by using different enrichment calculation methods. We focused on the same set of pre-selected genes as in RIP-chip experiments (Figure 4). First, we looked at the relative enriched RNA in Rim4 immunoprecipitates over background input (i.e., method (1), tagged immunoprecipitate over input from the same strain) (Figure 6C, Table 4). We observed a highly significant enrichment in the group of genes with delayed translation (the genes co-clustering with *CLB3* together with the genes co-clustering with *AMA1*) with respect to the group of negative control genes (p = 7.30E-09). Second, we looked at the relative enrichment of RNA from Rim4 tagged protein immunoprecipitates over untagged protein immunoprecipitates (Figure 6D). The group of genes with delayed translation again had a higher enrichment with respect to the group of negative control genes (p = 0.007).

Some highly enriched RNAs were not in our pre-selected groups. Some of them were translationally repressed, but did not co-cluster with *CLB3* or *AMA1*. Others did not have translational delay. Further studies are required to investigate the relationship between Rim4 and those genes.

Considering both RIP-chip and CLIP-seq results, it seems very likely that Rim4 co-immunoprecipitates mRNAs that have translational delays, supporting the hypothesis that Rim4 regulates translation of those genes by direct binding. No matter what methods we used to immunoprecipitate Rim4, and what methods to analyze data, we could always observe higher enrichment in the group of translationally repressed genes than the group of negative control genes, although the statistical significance level varied. In addition, if we compared the most reliable result from RIP-chip experiments (Figure 5B) and CLIP-seq experiments (Figure 6C), CLIP-seq experiments did exhibit a much clearer enrichment separation pattern

between translationally repressed genes and negative control genes, than RIP-chip

experiment. In agreement with the figures, the former (p = 7.30E-09) also had a much

smaller p-value than the latter (p = 0.02). This suggested an increased specificity in CLIP-seq

experiments.

Chapter 4

Discussion

4.1 How does Rim4 find its targets?

It is still unclear how Rim4 finds its targets. Motif searches have been done, but no significant motif has stood out. It is noteworthy that Rim4 has two RRMs. Each RRM might bind a different motif. In this case, it could be hard for the motif searching program to find a motif. Another possibility is that Rim4 might recognize a RNA secondary structure instead of a ribonucleotide motif. It is also possible that Rim4 mediates translational control through a complex. Rim4 may not directly associate with mRNAs of our interesting translationally repressed genes.

4.2 How does Ime2 regulate *CLB3* translation via Rim4?

Ime2 is a meiosis specific protein kinase, and phosphorylates Rim4 [2]. We are interested to investigate whether Ime2 kinase activity affects Rim4 binding affinity. It has been found [2] that in an *IME2st* strain, where Ime2 has higher protein expression and therefore kinase activity than in wild-type, that translational delay of *CLB3, GIP1 and SPS1* is lost in meiosis I. Clb3, Gip1 and Sps1 proteins are produced as soon as their RNAs are transcribed. At the same time, the Rim4 protein decreases earlier than in the wild-type strain. This evidence together suggests that Ime2 regulates Rim4 protein abundance to mediate *CLB3* translational repression. However, Ime2 might regulate Rim4 in other ways to regulate *CLB3* translation. In an *IME2st* strain, western blotting shows the accumulation of Clb3 protein even before

Rim4 protein significantly decreases [2]. This could be because Clb3 translation initiation is sensitive to a slight decrease in Rim4 protein. Or in a very small amount of cells, Rim4 decreases and Clb3 gets highly expressed [2]. But it is also possible that Ime2 phosphorylates Rim4 to impair its RNA binding ability, so as to relieve the translational repression of *CLB3*.

To test this possibility, CLIP-seq could be done on wild-type tagged Rim4 strain in an *IME2st* background at meiosis I. By looking at the RNAs co-immunoprecipitated with Rim4 in the *IME2st* background, we could tell whether increasing the Ime2 abundance and kinase activity would lead to RNA binding affinity change in Rim4.

4.3 Role of Rim4 in early meiosis

It would be very interesting to investigate the RNAs co-immunoprecipitated with Rim4 in early meiosis, since Rim4 probably binds RNA at the early stage. On the one hand, the *rim4* mutant has obvious phenotypes in early meiosis. Rim4 expression is induced in early meiosis, and dependent on Ime1. Homozygous *rim4* null mutation leads to a reduction in the level of *IME2* transcript [14]. The *rim4Δ* homozygous mutant is defective in premeiotic DNA synthesis [13]. Rim4 probably executes its early meiotic function through RNA binding. On the other hand, some early gene transcripts, including *CLB5* and *CLB6,* were highly enriched in Rim4 meiosis I immunoprecipitates identified by RIP-chip (Table 3). Since our meiosis culture was not fully synchronized, these early transcripts might come from the cells which did not enter meiosis I. In other words, they could be the Rim4 early meiosis targets, but included in the meiosis I target list because of the asynchrony.

Furthermore, *rim4* mutants share phenotypes with the *ime4* and *mum2* mutants [13,14]. Ime4 and Mum2 participate in RNA N^6- methyladenosine (m6A) modification, which is only present in meiotic transcripts, but not in vegetative transcripts [7–10]. Thus the meiotic RNA binding protein Rim4 might also play a role in m6A modification. This hypothesis could be tested by comparing the Rim4 early meiosis target list with the m6A target list.

4.4 Msa1: Rim4 homolog in *Schizosaccharomyces pombe*

Msa1 is the Rim4 homolog in fission yeast *S. pombe*. Interestingly, Msa1 and Rim4 are displaying opposite phenotype in meiosis. Rim4 is a meiotic activator in *S. cerevisae*. On the contrary, Msa1 inhibits sexual differentiation, and so inhibits meiosis, while the *msa1* mutant hypersporulates [21]. It would be very interesting to investigate the RNAs co-immunoprecipitated with Msa1 in *S. pombe*. Comparing Rim4 and Msa1 binding target lists might help to understand how homologous genes finally evolve to opposite functions.
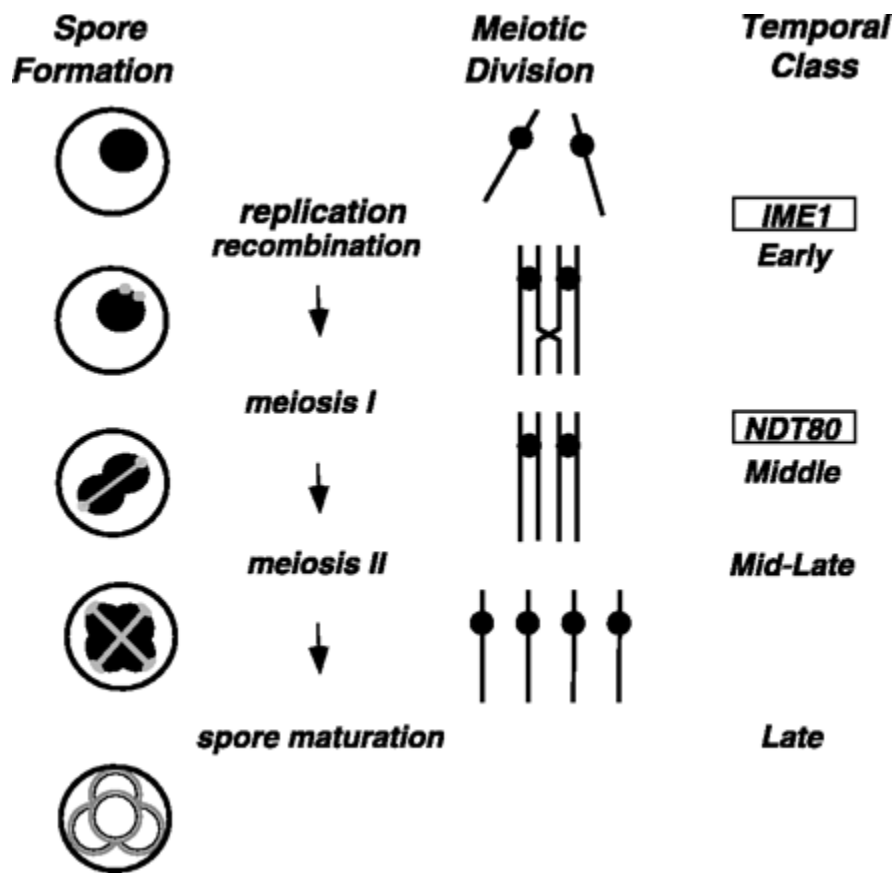
Figure 1 Yeast sporulation is regulated at the transcriptional level. This figure was obtained from Figure 1 in Chu *et al.,* 1998**.** Yeast sporulation involves two processes, meiosis and spore morphogenesis. The two processes are delicately coordinated and regulated at the transcriptional level by four major groups of genes: early, middle, mid-late and late genes.
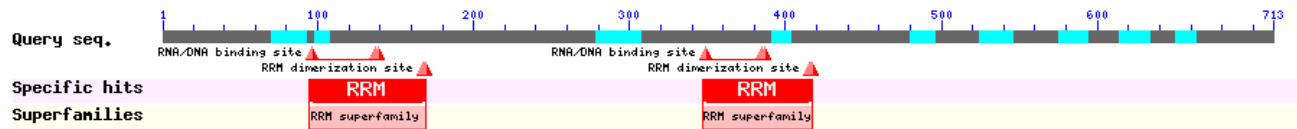
Figure 2 Rim4 has two RNA recognition motifs (RRMs). The figure was obtained from PubMed conserved domain database.
http://www.ncbi.nlm.nih.gov/Structure/cdd/wrpsb.cgi?seqinput=NP_011839.1
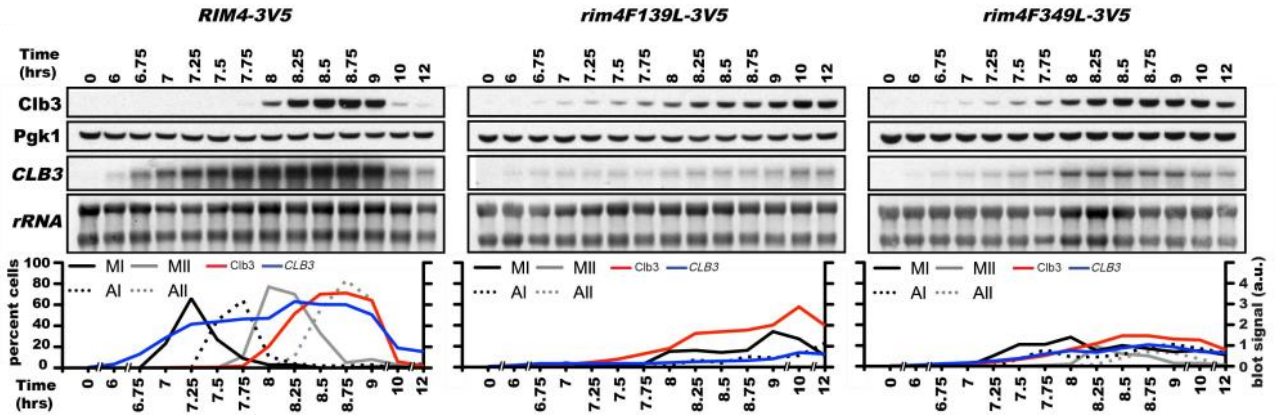
Figure 3 *rim4* RRM mutants knock out *CLB3* translational delay. This figure was obtained from Figure 5 in Berchowitz *et al*., 2013**.** A30868 (wild-type 3×V5 tagged Rim4, *RIM4-3V5*), A31420 (1st RRM mutated 3×V5 tagged *rim4*, *rim4-F139L-3V5*) and A31421 (2nd RRM mutated 3×V5 tagged *rim4*, *rim4-F349L-3V5*), harboring *GAL4.ER pGAL-NDT80* system (Carlile & Amon, 2008), were induced to meiosis. Upon addition of β-estradiol at 6h, cells were released from the Ndt80 block and continued meiotic progression synchronously. Cells were harvested at the time points as indicated, and Clb3 protein level and *CLB3* RNA level were examined. Blot quantification was shown in the lower panel.
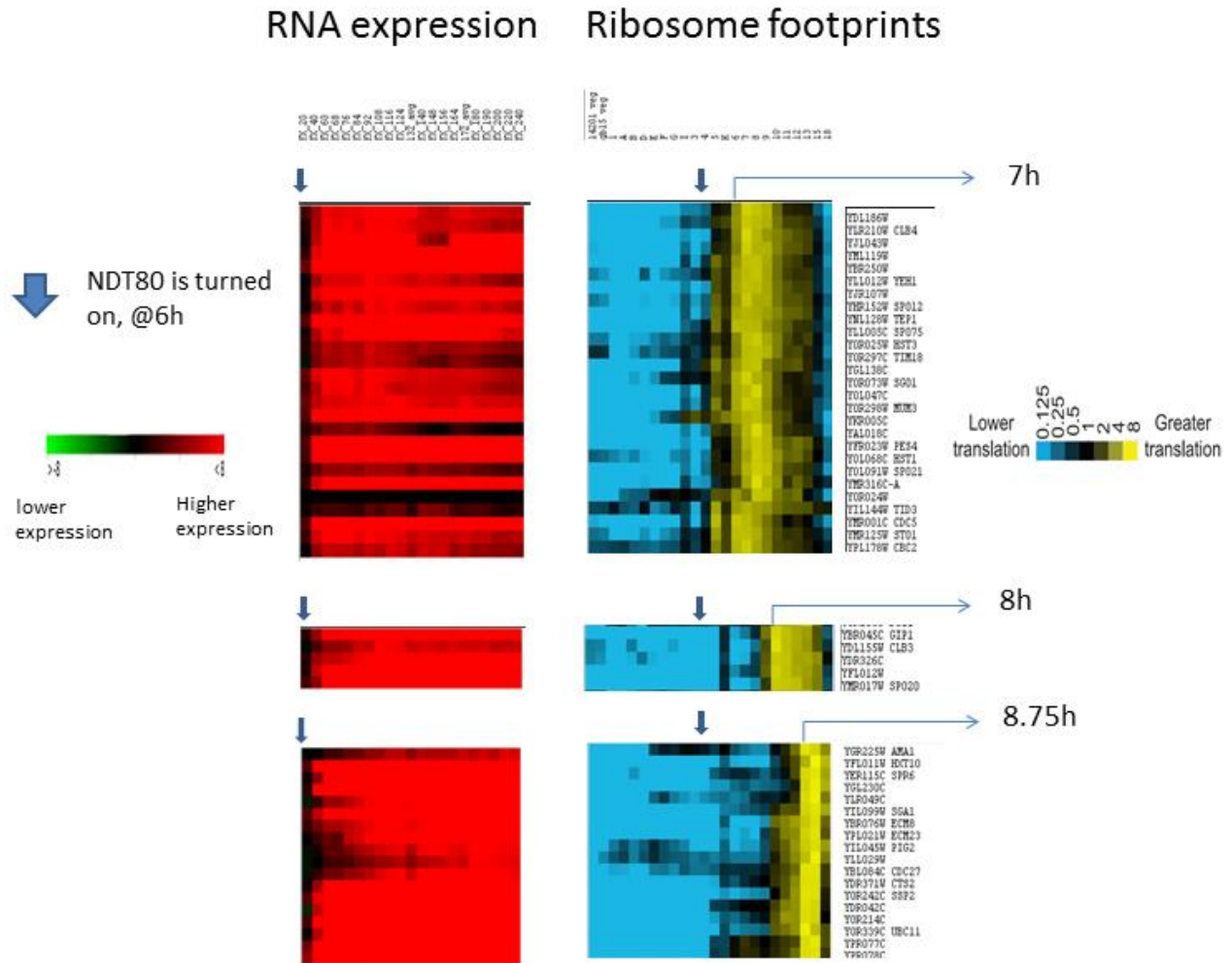
Figure 4 Translation is regulated in meiosis. Middle meiosis RNA expression data were extracted from Xu and Futcher's unpublished results, while footprint data were extracted from Brar *et al*., 2012. Blue arrow indicated the 6h time point when Ndt80 was turned on. RNA expression of all the three groups genes were quickly turned on after Ndt80 activation. However, their translation started at different time. Genes in the upper panel, that is, genes co-clutering with *CDC5* in the Brar footprint data, did not have obvious translational delay. Genes in the middle panel were the genes co-clustering with *CLB3* in the footprint data. Protein expression of these genes were repressed until 8h. Genes co-clustering with *AMA1* in the footprint data were grouped in the lower panel. These genes had even longer delay in protein translation. Footprint appeared at around 8.75h.

Figure 5 RIP-chip experiments were performed to identify the RNAs co-immunoprecipitated with Rim4 in meiosis I. (A) Western blot showed that tagged Rim4 was successfully pulled down. -: A15055 (wild-type untagged Rim4, *RIM4*); M: A31420 (1st RRM mutated 3×V5 tagged *rim4*, *rim4-F139L-3V5*); +: A30868 (wild-type 3×V5 tagged Rim4, *RIM4-3V5*); Lysate: input cell lysate before immunoprecipitation; Eluates: pooled solution after V5 peptide elution; Leftover on beads: protein left on beads after elution. (B) RNA specific enrichment was calculated by comparing wild-type tagged Rim4 strain (*RIM4-3V5*) with wild-type untagged strain (*RIM4*). x-axis showed the corresponding total RNA expression level in *RIM4-3V5*. (C) RNA specific enrichment was calculated by comparing wild-type tagged Rim4 strain (*RIM4-3V5*) with mutant tagged strain (*rim4-F139L-3V5)*. x-axis showed the corresponding total RNA expression level in *RIM4-3V5*.

A

B

C

- ● *CLB3*
- ● *SPO20, SPS1, GIP1, YSP2, YFL012W*
- ● Translationally repressed genes that co-cluster with *AMA1*
- ● Negative control pool

IP in *RIM-TAP* vs. input in *RIM-TAP*

D

- ● *CLB3*
- ● *SPO20, SPS1, GIP1, YSP2, YFL012W*
- ● Translationally repressed genes that co-cluster with *AMA1*
- ● Negative control pool
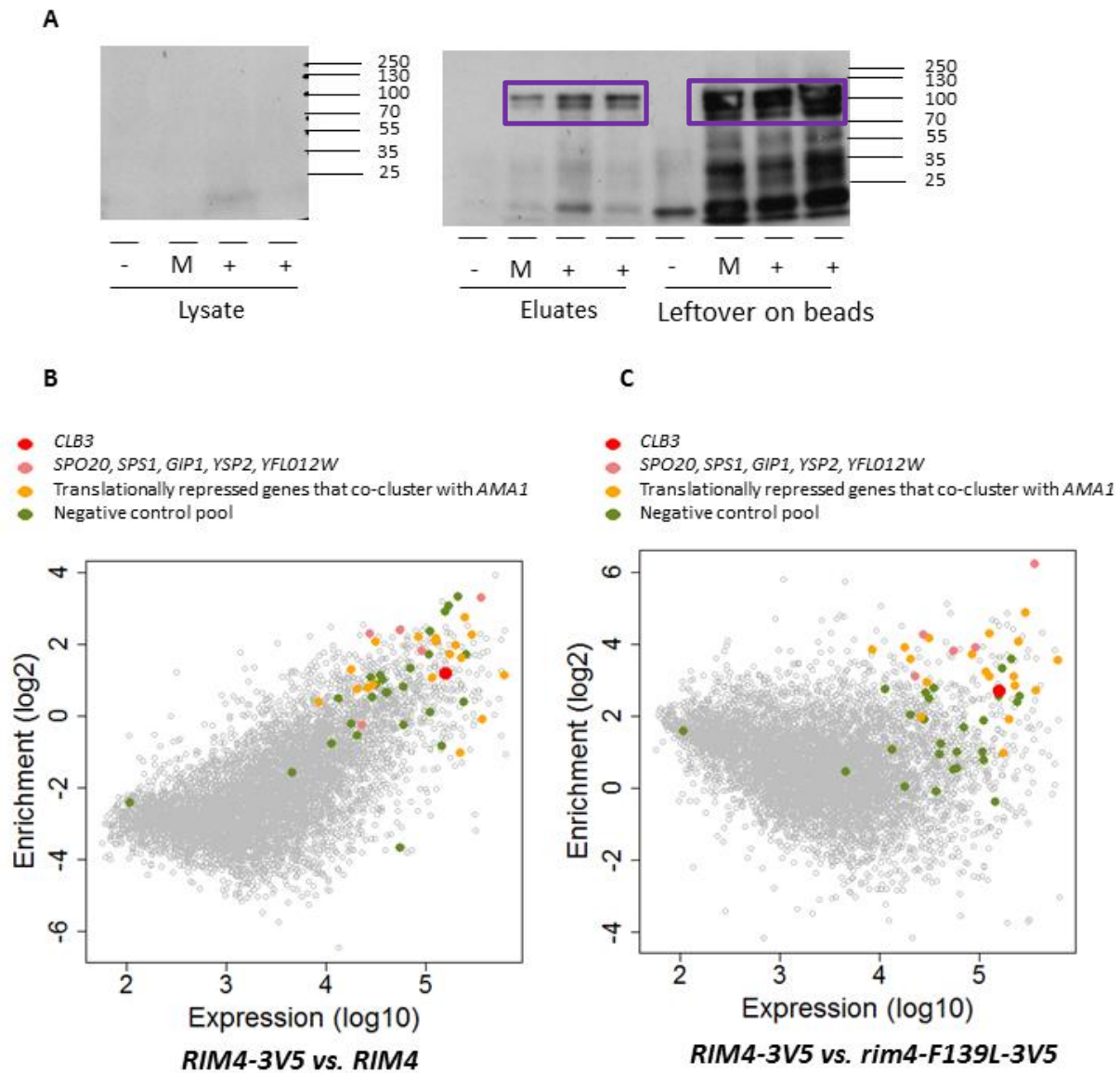
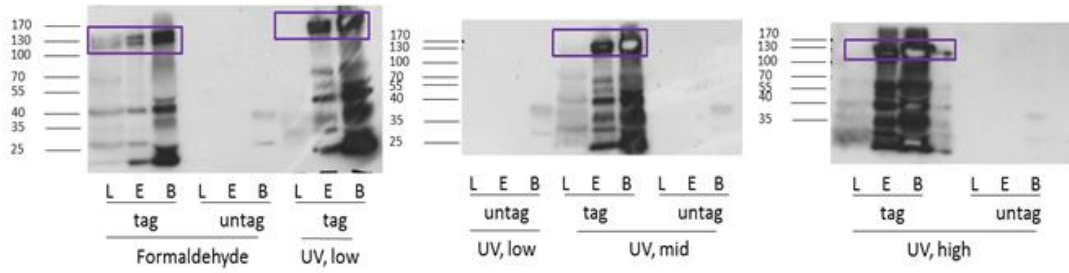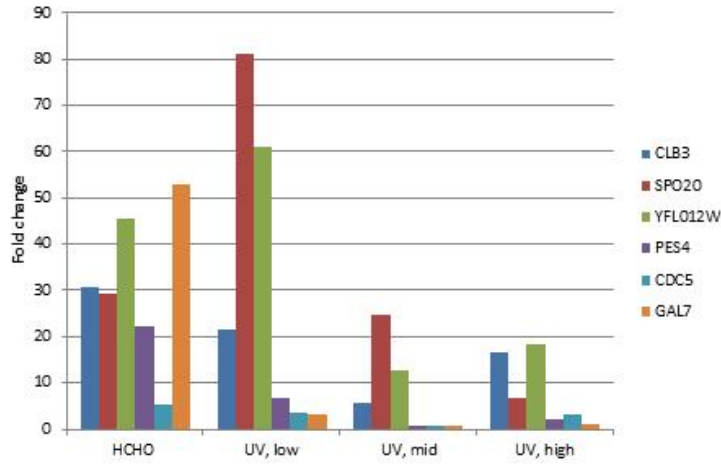

IP in *RIM-TAP* vs. IP in *RIM*

31
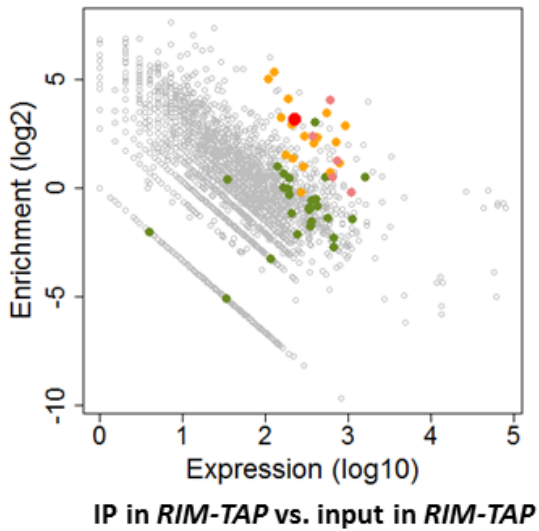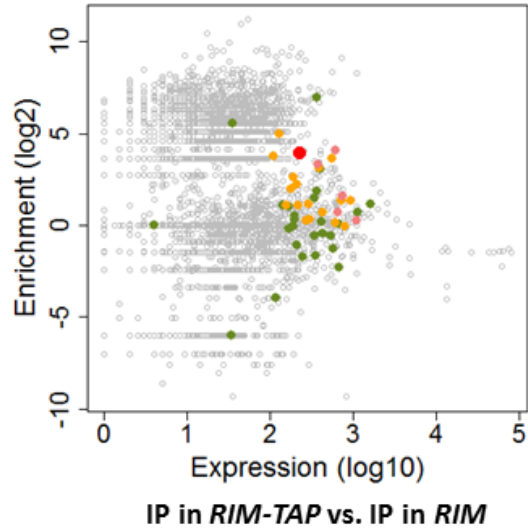
Figure 6 CLIP-seq experiments were performed to identify the RNAs co-immunoprecipitated with Rim4 in meiosis I. (A) Western blot showed that tagged Rim4 was successfully pulled down. untag: A14201 (wild-type untagged Rim4, *RIM4*); tag: CX6 (wild-type TAP tagged Rim4, *RIM4-TAP*); L: input cell lysate before immunoprecipitation; E: pooled solution after SDS elution; B: protein left on beads after elution; Formaldehyde: formaldehyde cross-linking; UV, low: UV cross-linking at the low dosage; UV, mid: UV cross-linking at the mid dosage; UV, high: UV cross-linking at the high dosage. (B) RNA enrichment fold change was examined by qPCR. *CLB3, SPO20, YFL012W, PES4, CDC5* and *GAL7* were tested. (C) RNA enrichment was calculated as the ratio of reads in IP sample over reads in input sample. Both samples were from wild-type tagged Rim4 strain (*RIM4-TAP)*. x-axis showed corresponding input reads in *RIM4-TAP*. (D) RNA enrichment was calculated as the ratio of reads in IP sample from wild-type tagged Rim4 strain (*RIM4-TAP)* over reads in IP sample from wild-type untagged strain (*RIM4)*. x-axis showed corresponding input reads in *RIM4-TAP*.

Table 1 Strains used in this study

Strain	Relevant genotype	Source
A15055	*MATa/MATalpha ura3::pGPD1-GAL4(848).ER::URA3/ura3::pGPD1-GAL4(848).ER::URA3 pGAL-NDT80::TRP1/pGAL-NDT80::TRP1 CLB3-3HA::KANMX6/CLB3-3HA::KANMX*	(Berchowitz et al., 2013)
A30868	*MATa/MATalpha ura3::pGPD1-GAL4(848).ER::URA3/ura3::pGPD1-GAL4(848).ER::URA3 pGAL-NDT80::TRP1/pGAL-NDT80::TRP1 CLB3-3HA::KANMX6/CLB3-3HA::KANMX6 RIM4-3V5::HIS3MX6/ RIM4-3V5::HIS3MX6*	(Berchowitz et al., 2013)
A31420	*MATa/MATalpha ura3::pGPD1-GAL4(848).ER::URA3/ura3::pGPD1-GAL4(848).ER::URA3 pGAL-NDT80::TRP1/pGAL-NDT80::TRP1 CLB3-3HA::KANMX6/CLB3-3HA::KANMX6 rim4-F139L-3V5/rim4-F139L-3V5*	(Berchowitz et al., 2013)
A14201	*MATa/MATalpha ura3::pGPD1-GAL4(848).ER::URA3/ura3::pGPD1-GAL4(848).ER::URA3 pGAL-NDT80::TRP1/pGAL-NDT80::TRP1*	(Carlile & Amon, 2008)
CX6	*MATa/MATalpha ura3::pGPD1-GAL4(848).ER::URA3/ura3::pGPD1-GAL4(848).ER::URA3 pGAL-NDT80::TRP1/pGAL-NDT80::TRP1 RIM4-TAP::kanMX6/ RIM4-TAP::kanMX6*	This study

Table 2 qPCR primers for CLIP

Gene	Primer	
CLB3	Forward	TGAGCTCTGGACACATCAGG
	Reverse	TTTAATTGGGGCGACTTTTG
SPO20	Forward	ATTATGGCTCACGCTTTTGG
	Reverse	CACCATCTTTTCCCGATCAC
YFL012W	Forward	AGCACAGATAGGATACGTAAGTGG
	Reverse	TCTCTTGAACATCCTACAAGAACA
PES4	Forward	AAATCCGGTCACAAGAATGG
	Reverse	AAGTAACCATGGCCCAGTGA
CDC5	Forward	CGCAGACCTCGTAGGAAAAG
	Reverse	TAATTTGGAAACAGCGAGCA
GAL7	Forward	CATCTGGCCATTTGAGACCT
	Reverse	ACCAGTCGCATTCAAAGGAG

Table 3 Top enriched genes in RIP-chip experiments

Rank	Gene	Enrichment ($\log_2$)*
1	YDR133C	3.93
2	PES4	3.34
3	SPO20	3.29
4	ACB1	3.19
5	STO1	3.07
6	YAL018C	2.90
7	YOR214C	2.77
8	SUT1	2.55
9	ICL1	2.54
10	YNL155W	2.50
11	SPR3	2.48
12	RAX2	2.48
13	GCN4	2.45
14	YFL012W	2.40
15	TMA17	2.39
16	GAL7	2.39
17	AAT2	2.39
18	YEH1	2.38
19	GAS4	2.34
20	HPF1	2.33
21	YSP2	2.31
22	CIT1	2.30
23	RPM2	2.27
24	SSP2	2.27
25	ZPS1	2.23
26	MUM2	2.23
27	HNT1	2.22
28	FET5	2.22
29	SGA1	2.20
30	SPO14	2.20
31	CLB5	2.17
32	CDA2	2.16
33	AMA1	2.15
34	SPS2	2.15
35	KAR2	2.15
36	BEM2	2.09
37	LPD1	2.07
38	ECM8	2.07
39	YDR042C	2.06

40	MRP8	2.05
41	FLO10	2.04
42	CCC2	2.04
43	GSC2	2.02
44	PCK1	2.02
45	JHD2	1.99
46	MIP6	1.99
47	COX7	1.98
48	YLR345W	1.98
49	HSP60	1.97
50	YGL230C	1.97
60	SPS1	1.81
158	CLB3	1.20
198	CLB6	1.03

*Enrichment is calculated as:

$$specific\ enrichment_{(Gene\ X)} = log_2 \frac{enrichment_{(WT\ tag,\ normalized,\ Gene\ X)}}{enrichment_{(WT\ untag,\ normalized,\ Gene\ X)}}$$

Table 4 Top enriched genes in CLIP-seq experiments

Rank	Gene	Enrichment ($\log_2$)**
1	RPL26B	7.61
2	DBP2	7.36
3	SLD2	7.04
4	RPL41A	6.89
5	RPL30	6.88
6	YBR191W-A	6.84
7	NSE1	6.84
8	YPL025C	6.74
9	RPS19B	6.69
10	YHR095W	6.66
11	YNL143C	6.59
12	MET7	6.59
13	TIR4	6.40
14	PCL5	6.39
15	CCW12	6.35
16	PAC10	6.30
17	YNL179C	6.28
18	NOB1	6.20
19	YMR325W	6.19
20	tP(UGG)A	6.11
21	PHO89	6.11
22	PFD1	6.11
23	EDC1	6.08
24	TIP1	6.01
25	YGR174W-A	5.99
26	YLR342W-A	5.95
27	BCS1	5.85
28	YLR111W	5.85
29	YOR387C	5.85
30	tI(AAU)E2	5.85
31	RPA43	5.83
32	YGL079W	5.82
33	YKR040C	5.77
34	YKR041W	5.77
35	RPL39	5.76
36	BUD19	5.76
37	CTS1	5.74
38	YLR286W-A	5.74
39	RPL29	5.74

40	RPS12	5.74
41	RPS4A	5.65
42	ALD6	5.65
43	RPL2B	5.64
44	YOL086W-A	5.64
45	RPL32	5.61
46	RPS9B	5.61
47	RPS16B	5.60
48	RPS17B	5.60
49	RPL37A	5.60
50	SHE1	5.60
51	RPL33A	5.55
52	YPL142C	5.55
53	TRS20	5.54
54	YCL026C-B	5.54
55	YCL001W-A	5.54
56	tS(AGA)E	5.54
57	YGR079W	5.54
58	YLR042C	5.54
59	ASP3-1	5.54
60	RKI1	5.54
61	YOR394W	5.54
62	NIP7	5.54
63	YLL055W	5.54
64	UTP6	5.51
65	YKR043C	5.49
66	RPL25	5.48
67	AAC1	5.47
68	RUF5-1	5.46
69	YHR052W-A	5.46
70	CUP1-1	5.46
71	MET14	5.39
72	HXT7	5.36
73	RPS22A	5.36
74	YLR099W-A	5.36
75	RPL36B	5.36
76	YPL250W-A	5.36
77	YMR175W-A	5.32
78	ECM8	5.31
79	YBR076C-A	5.31
80	tT(AGU)D	5.31

81	PRY1	5.30
82	RPS27B	5.29
83	ARX1	5.25
84	RPS7A	5.24
85	RPS31	5.22
86	YDR417C	5.22
87	RPL12B	5.22
88	YKL068W-A	5.22
89	TAN1	5.18
90	tH(GUG)G1	5.13
91	COG2	5.13
92	NSR1	5.13
93	YGR160W	5.13
94	YLL065W	5.13
95	YLR046C	5.13
96	ASP3-3	5.13
97	DUS4	5.13
98	YPR064W	5.13
99	RPS14A	5.12
100	RPL40B	5.12
284	SPO20	4.02
533	AMA1	3.45
594	CLB3	3.18

**Enrichment is calculated as:

$$enrichemnt_{(Gene\ X)} = log_2 \frac{Reads_{(WT\ tag,\ IP, Gene\ X)}}{Reads_{(WT\ tag, input,\ Gene\ X)}}$$

Reference

1. Brar, G. A. *et al.* High-resolution view of the yeast meiotic program revealed by ribosome profiling. *Science* **335,** 552–557 (2012).

2. Berchowitz, L. E. *et al.* A developmentally regulated translational control pathway establishes the meiotic chromosome segregation pattern. *Genes Dev.* **27,** 2147–2163 (2013).

3. Chu, S. *et al.* The Transcriptional Program of Sporulation in Budding Yeast. *Science* **282,** 699–705 (1998).

4. Lardenois, A. *et al.* Execution of the meiotic noncoding RNA expression program and the onset of gametogenesis in yeast require the conserved exosome subunit Rrp6. *Proc. Natl. Acad. Sci. U. S. A.* **108,** 1058–1063 (2011).

5. Chu, S. & Herskowitz, I. Gametogenesis in yeast is regulated by a transcriptional cascade dependent on Ndt80. *Mol. Cell* **1,** 685–696 (1998).

6. Primig, M. *et al.* The core meiotic transcriptome in budding yeasts. *Nat. Genet.* **26,** 415–423 (2000).

7. Schwartz, S. *et al.* High-resolution mapping reveals a conserved, widespread, dynamic mRNA methylation program in yeast meiosis. *Cell* **155,** 1409–1421 (2013).

8. Bodi, Z., Button, J. D., Grierson, D. & Fray, R. G. Yeast targets for mRNA methylation. *Nucleic Acids Res.* **38,** 5327–5335 (2010).

9.   Clancy, M. J., Shambaugh, M. E., Timpte, C. S. & Bokar, J. a. Induction of sporulation in Saccharomyces cerevisiae leads to the formation of N6-methyladenosine in mRNA: a potential mechanism for the activity of the IME4 gene. *Nucleic Acids Res.* **30,** 4509–4518 (2002).

10. Agarwala, S. D., Blitzblau, H. G., Hochwagen, A. & Fink, G. R. RNA methylation by the MIS complex regulates a cell fate decision in yeast. *PLoS Genet.* **8,** e1002732 (2012).

11. Wang, X. *et al.* N6-methyladenosine-dependent regulation of messenger RNA stability. *Nature* **505,** 117–120 (2014).

12. Wang, Y. *et al.* N6-methyladenosine modification destabilizes developmental regulators in embryonic stem cells. *Nat. Cell Biol.* **16,** 191–198 (2014).

13. Deng, C. & Saunders, W. S. RIM4 encodes a meiotic activator required for early events of meiosis in Saccharomyces cerevisiae. *Mol. Genet. Genomics* **266,** 497–504 (2001).

14. Soushko, M. & Mitchell, A. P. An RNA-binding protein homologue that promotes sporulation-specific gene expression in Saccharomyces cerevisiae. *Yeast* **16,** 631–639 (2000).

15. Carlile, T. M. & Amon, A. Meiosis I is established through division-specific translational control of a cyclin. *Cell* **133,** 280–291 (2008).

16. Hogan, D. J., Riordan, D. P., Gerber, A. P., Herschlag, D. & Brown, P. O. Diverse RNA-binding proteins interact with functionally related sets of RNAs, suggesting an extensive regulatory system. *PLoS Biol.* **6,** e255 (2008).

17. Cai, Y. & Futcher, B. Effects of the yeast RNA-binding protein Whi3 on the half-life and abundance of CLN3 mRNA and other targets. *PLoS One* **8,** e84630 (2013).

18. Selth, L. A., Gilbert, C. & Svejstrup, J. Q. RNA immunoprecipitation to determine RNA-protein associations in vivo. *Cold Spring Harb. Protoc.* **2009,** pdb.prot5234 (2009).

19. Darnell, R. CLIP (cross-linking and immunoprecipitation) identification of RNAs bound by a specific protein. *Cold Spring Harb. Protoc.* **2012,** 1146–1160 (2012).

20. Ule, J. *et al.* CLIP identifies Nova-regulated RNA networks in the brain. *Science* **302,** 1212–1215 (2003).

21. Jeong, H. T. *et al.* A novel gene, msa1, inhibits sexual differentiation in Schizosaccharomyces pombe. *Genetics* **167,** 77–91 (2004).